Published in IET Power Electronics
Received on 26th April 2010
Revised on 13th August 2010
doi: 10.1049/iet-pel.2010.0134

ISSN 1755-4535

# Non-linear optimal controller for unified power quality conditioners

*A.E. Leon*[1] *S.J. Amodeo*[1] *J.A. Solsona*[1] *M.I. Valla*[2]

[1]*Instituto de Investigaciones en Ingeniería Eléctrica (IIIE) 'Alfredo Desages' (UNS-CONICET), Departamento de Ingeniería Eléctrica y de Computadoras, Universidad Nacional del Sur, Avenida Alem 1253, Bahía Blanca, C.P. 8000, Argentina*
[2]*Laboratorio de Electrónica Industrial, Control e Instrumentación (LEICI), Facultad de Ingeniería, Universidad Nacional de La Plata and Consejo Nacional de Investigaciones Científicas y Técnicas (CONICET), La Plata, C.P.1900, Argentina*
*E-mail: andreseleon@gmail.com*

**Abstract:** A new optimal control strategy for unified power quality conditioners (UPQC) is presented. This strategy is based on feedback linearisation. The UPQC consists of series and shunt converters, where the series converter usually works as a voltage source, and the shunt converter works as a current source. However, it is possible to use the series converter as a current source, and the shunt converter as a voltage source, as utilised in this study. As for this scheme, an optimal voltage angle at load terminals, in order to minimise the converter losses, is proposed. A comparison with the traditional UPQC, where series and shunt converters are considered to be voltage and current sources, respectively, is also presented.

## 1 Introduction

The increasing use of loads based on power switching electronics makes non-sinusoidal currents flow in the power network so that non-sinusoidal voltage drops appear in the electrical system [1]. In addition, sags and swells in the voltage supply might provoke the malfunction in digital devices, medical and communication equipments and process controllers, which are highly sensitive to voltage disturbances and are becoming widely used in industrial applications. Moreover, regulatory agencies are demanding stricter power quality standards to diminish the reactive power and harmonics consumed by the loads. For these reasons, engineers need to improve the current solutions based on passive filters, which present load resonant effects, and only compensate pre-tuning frequencies. Therefore converter-based solutions are becoming increasingly common in industrial applications [2–9]. An integral solution to these power quality problems can be accomplished using the unified power quality conditioner (UPQC) [10].

The UPQC consists of two voltage-source converters (VSCs) connected to the network: one of them is in series, and the other one is in shunt. They are also inter-connected through a dc-link stage. This device provides to the load a regulated, flicker-free and harmonic-free voltage and, at the same time, eliminates current harmonics generated by the load. Accordingly the UPQC can present to the network a unity power factor load, while keeping the voltage in the dc-link controlled without an external energy store source. The UPQC is able to compensate abnormal network voltages irrespective of their duration when they are inside of the UPQC nominal capacity.

The UPQC can be implemented using two topologies that imply two different control philosophies. One of them, found in most of the bibliography [11–33], uses the series converter as a non-sinusoidal voltage source, and the shunt converter as a non-sinusoidal current source (which will be called UPQC$_A$). However, in [34–37], a new UPQC philosophy has been recently implemented, partially based on the idea developed in [38], which uses the shunt converter as a sinusoidal voltage source and the series converter as a sinusoidal current source (UPQC$_B$), showing several advantages against the traditional UPQC$_A$.

The UPQC$_A$ reference calculation presents a certain complexity because $p-q$ theory [39, 40] and filters are needed to obtain the non-sinusoidal reference signals generated by VSCs. These filters produce unwanted delays in the dynamic transient when either the UPQC compensates for the flicker or a big step in the load active power occurs [12, 15, 16, 19, 20, 41]. These drawbacks are not found in the UPQC$_B$, as it is not necessary to use filtered signals to obtain the VSC references. Thus, these references are simpler to calculate and a faster transient response can be attained.

The voltage angle at load terminals is a degree of freedom in the UPQC control design. Then, this angle can be chosen to minimise a UPQC loss index, as is proposed in [20–24, 42] with regard to the UPQC$_A$. However to the best knowledge of the authors, UPQC$_B$ optimisation studies have not been reported yet.

The UPQC can be modelled as a seventh-order, non-linear and under-actuated system. It presents input-state products, and seven states are to be controlled by only four inputs. Different control strategies have been proposed in case of the UPQC$_A$. Among others, several control techniques based on linearisation around an operation point [11–13],

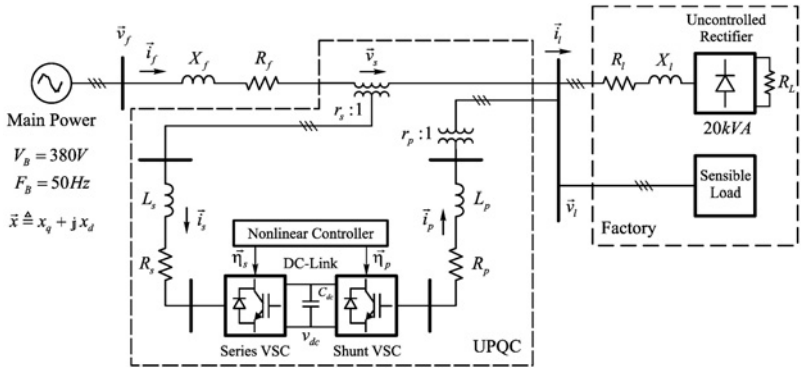


**Fig. 1** *General electric circuit of the UPQC, VSCs, load, and power network*

$H_\infty$ control [14], and unstructured neural networks and fuzzy logic strategies [15, 16] were used. However, as mentioned above, the nature of UPQC model is non-linear and structured; as a consequence non-linear control techniques, such as passivity-based control and sliding-mode control, have been introduced in [17, 18], respectively.

In this work, with the aim of obtaining a high-performance behaviour in the entire operation range of the UPQC, a non-linear control strategy, feedback linearisation control, is used in UPQC$_A$ and UPQC$_B$ topologies. In addition, control laws include a feedforward compensation of the load current and network voltage variations, in order to improve the dynamic response of the strategies. In addition, an optimal criterion to minimise UPQC$_B$ losses is presented. A comparison between both control philosophies is also accomplished.

The paper is organised as follows. In Section 2 UPQC models are shown. Optimal criteria are introduced in Section 3, then control strategies with regard to UPQC$_A$ and UPQC$_B$ are designed in Sections 4 and 5, respectively. Section 6 summarises the main differences between the two UPQC topologies. In Section 7, a performance assessment and discussions are presented. Finally conclusions are drawn in Section 8.

## 2 UPQC dynamic model

This section presents, with regard to both topologies, the UPQC mathematical model to be used in the sequel. The considered electrical circuit is a three-phase three-wire system. A general electric circuit of the UPQC internal connections, VSCs, the load and the power network is shown in Fig. 1.

### 2.1 Topology A

Fig. 2 shows the electrical topology of the UPQC$_A$. It can be seen that the shunt VSC is connected to the line through an inductance, where it then works as a current source. On the other hand, the series VSC is connected to the line by capacitors, where it works as a voltage source. This is the traditional UPQC scheme (UPQC$_A$). By using the Kirchhoff laws in the electrical circuits of Fig. 2, the following dynamic model in a $d$–$q$ rotating reference frame in per unit can be obtained [11, 13]

$$\frac{L_s}{\Omega_B}\frac{\mathrm{d}i_{sd}}{\mathrm{d}t} = -R_s i_{sd} - L_s \omega i_{sq} - \eta_{sd} v_{\mathrm{dc}} - r_s v_{sd} \tag{1}$$

$$\frac{L_s}{\Omega_B}\frac{\mathrm{d}i_{sq}}{\mathrm{d}t} = -R_s i_{sq} + L_s \omega i_{sd} - \eta_{sq} v_{\mathrm{dc}} - r_s v_{sq} \tag{2}$$

$$\frac{C_s r_s}{\Omega_B}\frac{\mathrm{d}v_{sd}}{\mathrm{d}t} = -C_s r_s \omega v_{sq} + i_{sd} - \frac{1}{r_s}(i_{ld} - r_p i_{pd}) \tag{3}$$

$$\frac{C_s r_s}{\Omega_B}\frac{\mathrm{d}v_{sq}}{\mathrm{d}t} = C_s r_s \omega v_{sd} + i_{sq} - \frac{1}{r_s}(i_{lq} - r_p i_{pq}) \tag{4}$$

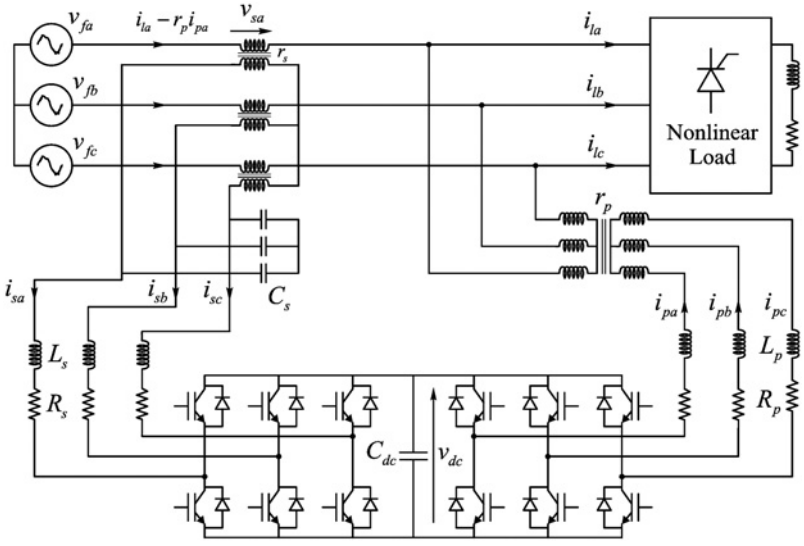


**Fig. 2** *Electrical circuit of the UPQC using topology A*




doi: 10.1049/iet-pel.2010.0134

$$\frac{L_p}{\Omega_B}\frac{\mathrm{d}i_{pd}}{\mathrm{d}t} = -R_p i_{pd} - L_p \omega i_{pq} + \eta_{pd} v_{\mathrm{dc}} - r_p(v_{fd} + v_{sd}) \quad (5)$$

$$\frac{L_p}{\Omega_B}\frac{\mathrm{d}i_{pq}}{\mathrm{d}t} = -R_p i_{pq} + L_p \omega i_{pd} + \eta_{pq} v_{\mathrm{dc}} - r_p(v_{fq} + v_{sq}) \quad (6)$$

$$\frac{C_{\mathrm{dc}}}{\Omega_B}\frac{\mathrm{d}v_{\mathrm{dc}}}{\mathrm{d}t} = (\eta_{sd} i_{sd} + \eta_{sq} i_{sq}) - (\eta_{pd} i_{pd} + \eta_{pq} i_{pq}) \quad (7)$$

In Fig. 2 and Table 1 variables and parameters are defined; $\eta_s$ and $\eta_p$ are the control inputs of the series and shunt VSCs, respectively. They represent the duty cycles of each converter.

### 2.2 Topology B

Fig. 3 shows the electrical topology of the UPQC$_B$. In this case, the shunt VSC is connected to the line through capacitors, where it then works as a voltage source. On the other hand, the series VSC is connected to the line by inductances, where then it works as a current source. Note that electrical circuits of the UPQC$_A$ and UPQC$_B$ devices are very similar. They only differ in which branch the capacitors are placed. As done before, it is possible to obtain the UPQC$_B$ dynamic model in a $d-q$ rotating reference frame using the Kirchhoff laws in the circuits of Fig. 3 [34, 35].

$$\frac{L_s}{\Omega_B}\frac{\mathrm{d}i_{sd}}{\mathrm{d}t} = \frac{r_s(v_{ld} - v_{fd})}{2} - \frac{r_s(v_{lq} - v_{fq})}{2\sqrt{3}} - R_s i_{sd} - L_s \omega i_{sq} - \eta_{sd} v_{\mathrm{dc}} \quad (8)$$

$$\frac{L_s}{\Omega_B}\frac{\mathrm{d}i_{sq}}{\mathrm{d}t} = \frac{r_s(v_{lq} - v_{fq})}{2} + \frac{r_s(v_{ld} - v_{fd})}{2\sqrt{3}} - R_s i_{sq} + L_s \omega i_{sd} - \eta_{sq} v_{\mathrm{dc}} \quad (9)$$

$$\frac{L_p}{\Omega_B}\frac{\mathrm{d}i_{pd}}{\mathrm{d}t} = \frac{r_p v_{ld}}{2} - \frac{r_p v_{lq}}{2\sqrt{3}} - R_p i_{pd} - L_p \omega i_{pq} + \eta_{pd} v_{\mathrm{dc}} \quad (10)$$

$$\frac{L_p}{\Omega_B}\frac{\mathrm{d}i_{pq}}{\mathrm{d}t} = \frac{r_p v_{lq}}{2} + \frac{r_p v_{ld}}{2\sqrt{3}} - R_p i_{pq} + L_p \omega i_{pd} + \eta_{pq} v_{\mathrm{dc}} \quad (11)$$

**Table 1** Parameters and data of devices

| Description | Parameter value | | Unit |
|---|---|---|---|
| *Power system* | | | |
| rated power | $S_N$ | 20 | kVA |
| base voltage (peak line-to-neutral value) | $V_B$ | $\sqrt{2} \times 220$ | V |
| base current (peak value) | $I_B$ | 42.85 | A |
| base angular frequency | $\Omega_B$ | $2\pi \times 50$ | Hz |
| dc-link voltage | $v_{\mathrm{dc}}$ | 630 | V |
| *UPQC data* | | | |
| shunt VSC resistance | $R_p$ | 0.01 | Ω |
| shunt VSC inductance | $L_p$ | 0.5 | mH |
| shunt VSC capacitance | $C_p$ | 75 | μF |
| series VSC resistance | $R_s$ | 0.1 | Ω |
| series VSC inductance | $L_s$ | 2 | mH |
| series VSC capacitance | $C_s$ | 75 | μF |
| relation of transformation (shunt VSC) | $r_p$ | 1:1 | – |
| relation of transformation (series VSC) | $r_s$ | 2:1 | – |
| dc-link bus capacitance | $C_{\mathrm{dc}}$ | 2200 | μF |
| HPF cut-off frequency | $\omega_{ch}$ | 25 | r/s |
| LPF cut-off frequency | $\omega_{cl}$ | 50 | r/s |
| switching frequency | $f_{\mathrm{sw}}$ | 15 | kHz |
| computational delay | $T_s$ | 70 | μs |
| *UPQC$_A$ controller gains* | | | |
| proportional gain of $v_s$ control | $K_{vs}$ | 2500 | pu |
| time constant of $v_s$ control | $T_{ivs}$ | 0.1 | pu |
| proportional gain of $i_p$ control | $K_{ip}$ | 6000 | pu |
| time constant of $i_p$ control | $T_{iip}$ | 0.15 | pu |
| proportional gain of $i_s$ control | $K_{is}$ | 2000 | pu |
| time constant of $i_s$ control | $T_{iis}$ | 0.0 | pu |
| proportional gain of $v_{\mathrm{dc}}$ control | $K_{\mathrm{dc}}$ | 100 | pu |
| time constant of $v_{\mathrm{dc}}$ control | $T_{i\mathrm{dc}}$ | 0.07 | pu |
| *UPQC$_B$ controller gains* | | | |
| proportional gain of $v_l$ control | $K_{vl}$ | 5000 | pu |
| time constant of $v_l$ control | $T_{ivl}$ | 0.1 | pu |
| proportional gain of $i_p$ control | $K_{ip}$ | 3500 | pu |
| time constant of $i_p$ control | $T_{iip}$ | 0.0 | pu |
| proportional gain of $i_s$ control | $K_{is}$ | 300 | pu |
| time constant of $i_s$ control | $T_{iis}$ | 0.05 | pu |
| proportional gain of $v_{\mathrm{dc}}$ control | $K_B$ | 3.7 | pu |
| time constant of $v_{\mathrm{dc}}$ control | $T_{iB}$ | 0.03 | pu |

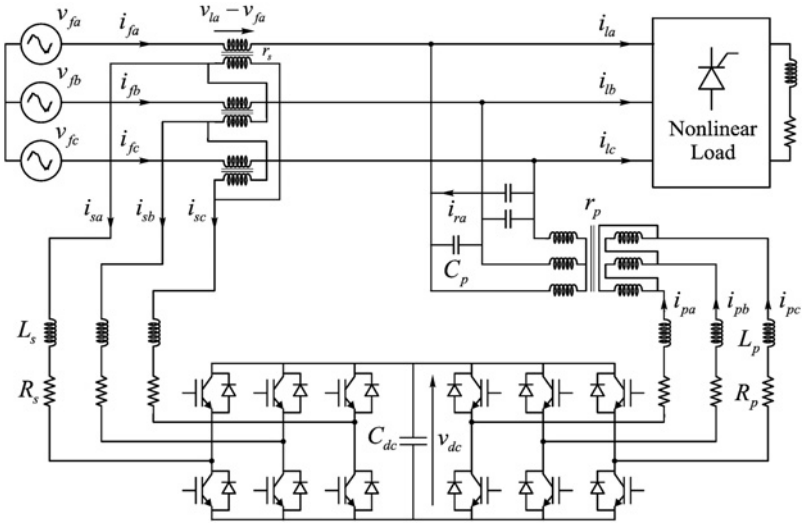


**Fig. 3** *Electrical circuit of the UPQC using topology B*

$$\frac{3C_p}{\Omega_B}\frac{dv_{ld}}{dt} = -\frac{r_s i_{sd}}{2} - \frac{r_s i_{sq}}{2\sqrt{3}} - \frac{r_p i_{pd}}{2} - \frac{r_p i_{pq}}{2\sqrt{3}} - i_{ld} - 3C_p \omega v_{lq} \quad (12)$$

$$\frac{3C_p}{\Omega_B}\frac{dv_{lq}}{dt} = -\frac{r_s i_{sq}}{2} + \frac{r_s i_{sd}}{2\sqrt{3}} - \frac{r_p i_{pq}}{2} + \frac{r_p i_{pd}}{2\sqrt{3}} - i_{lq} + 3C_p \omega v_{ld} \quad (13)$$

$$\frac{C_{dc}}{\Omega_B}\frac{dv_{dc}}{dt} = (\eta_{sd} i_{sd} + \eta_{sq} i_{sq}) - (\eta_{pd} i_{pd} + \eta_{pq} i_{pq}) \quad (14)$$

where variables and parameters can be seen in Fig. 3 and Table 1.

## 3 Optimal control philosophy

Since the voltage angle at load terminals, $\theta_L$, is a degree of freedom of the UPQC, it can be adjusted with the aim of working in an optimal operation point, in the sense of minimising converter losses. As is explained in [21], UPQC losses are determined by currents that flow in the series and shunt converters, $I_S$ and $I_P$, respectively, and by the dc-bus voltage $v_{dc}$. The $I_S$ current is governed by the load and by the relation of transformation $r_s$ chosen in the series transformer and by assumption of a dc-bus voltage set by the converter type. Then, the only way of acting on the UPQC losses will be through minimisation of the current of the shunt converter, $I_P$ [21]. Fig. 4 shows the relation between current vectors and the $\theta_L$ angle in the case of both topologies. The triangle (UPQC$_A$ case) and quadrangle (UPQC$_B$ case) of currents are built by applying the first Kirchhoff law at the connection point of the shunt converter.

It is important to note that in both topologies the increase in the load voltage angle, $\theta_L$, in order to minimise the $I_P$ current, results in an increase in the voltage injected by the series converter. Therefore the maximum optimal operation range is determined by the nominal voltage of the series transformer.

### 3.1 Traditional topology (UPQC$_A$ case)

From Fig. 4*a* the current vector amplitude in the shunt converter can be written as

$$I_P^2 = I_F^2 + I_L^2 - 2I_F I_L \cos(\phi - \theta_L) \quad (15)$$

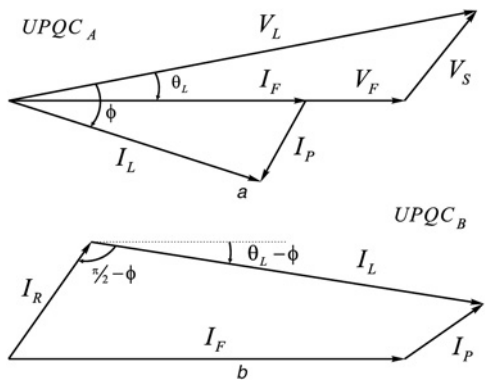


**Fig. 4** *Relations of current vectors at the connection point of the shunt converter*

*a* UPQC$_A$ topology
*b* UPQC$_B$ topology

In (15), it can be seen that in order to minimise the $I_P$ current, the voltage angle at load terminals must be set in the following optimal value:

$$\theta_L^\star = \phi \quad (16)$$

where $\cos(\phi)$ is the load power factor. This power factor can be computed from the load current and voltage measurements using the generalised theory of the instantaneous active and reactive power [39]. Additionally, a low-pass filter is included to calculate the output of the $\theta_L^\star$ angle in order to eliminate sudden variations in the phase reference. This factor prevents harmonic influence and allows one to track the $\theta_L^\star$ angle in an average value, avoiding load voltage distortions. In tests, a first-order low-pass filter with a cut-off frequency of $\omega_{cl} = 50\,\text{r/s}$ will be used.

### 3.2 New topology (UPQC$_B$ case)

The current geometry of the topology B is presented in Fig. 4*b*. By applying trigonometric relationships, it is possible to obtain the equation shown below, which relates the $I_P$ current with the $\theta_L$ angle.

$$I_P^2 = (I_F - I_L\cos(\theta_L - \phi) + I_R \sin\theta_L)^2 + (I_R \cos\theta_L + I_L \sin(\theta_L - \phi))^2 \quad (17)$$

The optimal value, $\theta_L^\star$, which minimises the shunt VSC current is obtained by verifying

$$\left.\frac{\partial I_P^2}{\partial \theta_L}\right|_{\theta_L^\star} = 2I_F(I_R \cos\theta_L^\star + I_L \sin(\theta_L^\star - \phi)) = 0 \quad (18)$$

$$\left.\frac{\partial^2 I_P^2}{\partial \theta_L^2}\right|_{\theta_L^\star} = 2I_F(I_L \cos(\theta_L^\star - \phi) - I_R \sin\theta_L^\star) > 0 \quad (19)$$

Finally from (18) and (19), it is possible to calculate the optimal load voltage angle of the UPQC$_B$ topology, yielding

$$\theta_L^\star = \arccos\left(\frac{I_L \cos\phi}{\sqrt{I_L^2 + I_R^2 - 2I_L I_R \sin\phi}}\right) \quad (20)$$

## 4 Control strategy for UPQC$_A$

### 4.1 Instantaneous active and reactive power theory

Using the generalised theory of the instantaneous active and reactive power [39], often called the $p$–$q$ theory, it is possible to define the following transformations to convert $d$–$q$ reference frame currents and voltages in instantaneous powers [41, 43, 44]

$$\begin{bmatrix} p \\ q \end{bmatrix} = \begin{bmatrix} v_d & v_q \\ -v_q & v_d \end{bmatrix}\begin{bmatrix} i_d \\ i_q \end{bmatrix} = \boldsymbol{T}_{ip}\boldsymbol{i} \quad (21)$$




doi: 10.1049/iet-pel.2010.0134

whereas the inverse transformation is given by

$$\begin{bmatrix} i_d \\ i_q \end{bmatrix} = \begin{bmatrix} \dfrac{v_d}{v_d^2+v_q^2} & \dfrac{-v_q}{v_d^2+v_q^2} \\ \dfrac{v_q}{v_d^2+v_q^2} & \dfrac{v_d}{v_d^2+v_q^2} \end{bmatrix} \begin{bmatrix} p \\ q \end{bmatrix} = \boldsymbol{T}_{pi}\boldsymbol{p} \tag{22}$$

The above shown transformations are going to be used in what follows.

### 4.2 Input transformation

Feedback linearisation control theory [45] is a powerful tool in controlling coupled non-linear systems. This technique achieves high performance tracking by choosing auxiliary control inputs in a particular way [4, 46]. In the case under study, the auxiliary control inputs shown below are going to be used to accomplish an exact linearisation in the entire operation range and transform the original system in a linear decoupled one. Auxiliary control inputs are defined as

$$u_{sd} \triangleq \frac{\Omega_B}{L_s}(-R_s i_{sd} - L_s \omega i_{sq} - \eta_{sd} v_{\rm dc} - r_s v_{sd}) \tag{23}$$

$$u_{sq} \triangleq \frac{\Omega_B}{L_s}(-R_s i_{sq} + L_s \omega i_{sd} - \eta_{sq} v_{\rm dc} - r_s v_{sq}) \tag{24}$$

$$u_{vd} \triangleq \frac{\Omega_B}{C_s r_s}\left(-C_s r_s \omega v_{sq} + i_{sd} - \frac{1}{r_s}(i_{ld} - r_p i_{pd})\right) \tag{25}$$

$$u_{vq} \triangleq \frac{\Omega_B}{C_s r_s}\left(C_s r_s \omega v_{sd} + i_{sq} - \frac{1}{r_s}(i_{lq} - r_p i_{pq})\right) \tag{26}$$

$$u_{pd} \triangleq \frac{\Omega_B}{L_p}(-R_p i_{pd} - L_p \omega i_{pq} + \eta_{pd} v_{\rm dc} - r_p(v_{fd} + v_{sd})) \tag{27}$$

$$u_{pq} \triangleq = \frac{\Omega_B}{L_p}(-R_p i_{pq} + L_p \omega i_{pd} + \eta_{pq} v_{\rm dc} - r_p(v_{fq} + v_{sq})) \tag{28}$$

$$u_{\rm dc} \triangleq \frac{\Omega_B}{C_{\rm dc}}((\eta_{sd} i_{sd} + \eta_{sq} i_{sq}) - (\eta_{pd} i_{pd} + \eta_{pq} i_{pq})) \tag{29}$$

By replacing the auxiliary control inputs (23)–(29) in the UPQC$_A$ system, (1)–(7), the following transformed system is obtained

$$\begin{aligned} \frac{{\rm d}i_{sd}}{{\rm d}t} &= u_{sd}, & \frac{{\rm d}i_{sq}}{{\rm d}t} &= u_{sq} \\ \frac{{\rm d}v_{sd}}{{\rm d}t} &= u_{vd}, & \frac{{\rm d}v_{sq}}{{\rm d}t} &= u_{vq} \\ \frac{{\rm d}i_{pd}}{{\rm d}t} &= u_{pd}, & \frac{{\rm d}i_{pq}}{{\rm d}t} &= u_{pq} \\ \frac{{\rm d}v_{\rm dc}}{{\rm d}t} &= u_{\rm dc} \end{aligned} \tag{30}$$

In this way the new system consists of seven first-order linear systems, fully actuated and decoupled from each other. This makes the control law design easier as it is to be developed in the following subsections.

### 4.3 Digital implementation to obtain the auxiliary control signals

Dynamic systems (30) can be characterised by the general form of a linear integrator, ${\rm d}x/{\rm d}t = u$. Then, by defining the tracking error as $e = x - x^\star$, a linear proportional plus integral (PI) regulator can be used to control the $x$ states and to obtain the auxiliary control signals, $u$

$$U(s) = \left(K + \frac{K}{T_i s}\right)E(s) \tag{31}$$

where the superscript '$\star$' denotes a desired reference value. A time-domain representation of the above Laplace transfer function is

$$u = -K(x - x^\star) - \frac{K}{T_i}\int (x - x^\star)\,{\rm d}t \tag{32}$$

To take into account the computational and processing delay the following procedure is performed. Fig. 5 shows the structure of a generic control loop where the linear regulator, computational delay, non-linear plant, feedback linearisation, actual and auxiliary controls are presented. The proportional gain, $K$, and time constant, $T_i$, of the PI regulator are designed to stabilise the closed loop shown in Fig. 5, in the same way as is accomplished in Section 5 of reference [47]. In order to be able to implement the dynamic part of the controller, in a digital processor, a discrete expression is needed. To obtain a discrete $z$-domain representation from continuous $s$-domain transfer functions, the bilinear transformation or Tustin approximation [48] was used, resulting in

$$s = \frac{2}{T_s}\frac{z-1}{z+1} \tag{33}$$

The proposed control algorithms were embedded and tested on a 32-bit float-point Texas Instrument TMS320F28335 digital signal controller. The time needed to run the algorithms was approximately 60 μs. Thus, the sample time is set to $T_{\rm s} = 70$ μs. Consequently, despite the complexity of the control laws, the proposed strategies can be implemented with actual digital processors available for these applications.

### 4.4 Injected voltage control of the series VSC

The voltage reference in the series VSC ($v_s^\star$) should be computed to obtain a harmonic- and flicker-free voltage whose amplitude equals to one at the load terminal ($V_L = 1$ pu). In addition, the load terminal voltage must have the phase determined by the loss minimisation

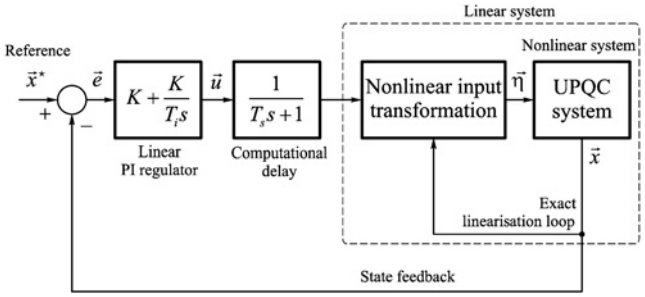


**Fig. 5** *Block diagram of the closed loop to obtain the auxiliary control signals*

criterion from (16). Therefore

$$v^{\star}_{sdq} = \begin{bmatrix} v^{\star}_{sd} & v^{\star}_{sq} \end{bmatrix}^{\mathrm{T}} = \begin{bmatrix} V_L \sin\theta^{\star}_L - v_{fd} & V_L \cos\theta^{\star}_L - v_{fq} \end{bmatrix}^{\mathrm{T}} \quad (34)$$

Then, using these voltage references, it is possible to calculate the auxiliary control inputs, $u_{vd}$ and $u_{vq}$, from the general procedure explained in Subsection 4.3. In this particular case, from (32), the following expressions result

$$u_{vd} = -K_{vs}(v_{sd} - v^{\star}_{sd}) - \frac{K_{vs}}{T_{ivs}}\int (v_{sd} - v^{\star}_{sd})\mathrm{d}t \quad (35)$$

$$u_{vq} = -K_{vs}(v_{sq} - v^{\star}_{sq}) - \frac{K_{vs}}{T_{ivs}}\int (v_{sq} - v^{\star}_{sq})\mathrm{d}t \quad (36)$$

### 4.5 Inner current control of the series VSC

The $i_s$ current control is an inner control loop that allows one to control the $v_s$ outer voltage loop in a cascade manner. Its references are obtained from (25) and (26)

$$i^{\star}_{sd} = C_s r_s \omega v_{sq} + \frac{1}{r_s}(i_{ld} - r_p i_{pd}) + \frac{C_s r_s}{\Omega_B} u_{vd} \quad (37)$$

$$i^{\star}_{sq} = -C_s r_s \omega v_{sd} + \frac{1}{r_s}(i_{lq} - r_p i_{pq}) + \frac{C_s r_s}{\Omega_B} u_{vq} \quad (38)$$

where (35) and (36) are needed. Then, from the above current references, the auxiliary control inputs $u_{sd}$ and $u_{sq}$ can be calculated in a similar way to (35) and (36), resulting in

$$u_{sd} = -K_{is}(i_{sd} - i^{\star}_{sd}) - \frac{K_{is}}{T_{iis}}\int (i_{sd} - i^{\star}_{sd})\,\mathrm{d}t \quad (39)$$

$$u_{sq} = -K_{is}(i_{sq} - i^{\star}_{sq}) - \frac{K_{is}}{T_{iis}}\int (i_{sq} - i^{\star}_{sq})\,\mathrm{d}t \quad (40)$$

### 4.6 Non-linear transformation to obtain the insulated gate bipolar transistor (IGBT) gate driving signals

The original control input $\eta_s$, which represents the duty cycle of the series VSC, can be recovered from (23) and (24), yielding

$$\eta_{sd} = \frac{1}{v_{\mathrm{dc}}}\left(-R_s i_{sd} - L_s \omega i_{sq} - r_s v_{sd} - \frac{L_s u_{sd}}{\Omega_B}\right) \quad (41)$$

$$\eta_{sq} = \frac{1}{v_{\mathrm{dc}}}\left(-R_s i_{sq} + L_s \omega i_{sd} - r_s v_{sq} - \frac{L_s u_{sq}}{\Omega_B}\right) \quad (42)$$

where (39) and (40) are needed.

Finally actual IGBT gate driving signals are obtained via a pulse width modulator with inputs $\eta_{sd}$ and $\eta_{sq}$. The amplitude and phase required for the space-vector modulation (SVM) stage are calculated as [49]

$$m = \sqrt{\eta^2_{sd} + \eta^2_{sq}} \quad (43)$$

$$\delta = \arctan(\eta_{sd}, \eta_{sq}) \quad (44)$$

### 4.7 Current control of the shunt VSC

The powers to be compensated, which are therefore generated by the shunt VSC will be: the oscillating component of active and reactive powers (with the aim of eliminating harmonics in the current) and the average reactive power consumed by the load (achieving a unity power factor). Then, the reference current calculation in the case of the shunt converter will be obtained by applying the transformation (22). It gives currents from powers and voltages. Thus

$$r_p \begin{bmatrix} i^{\star}_{pd} \\ i^{\star}_{pq} \end{bmatrix} = \boldsymbol{T}_{pi} \begin{bmatrix} \tilde{p} \\ q \end{bmatrix} = \frac{1}{v^2_{ld} + v^2_{lq}} \begin{bmatrix} v_{ld} & -v_{lq} \\ v_{lq} & v_{ld} \end{bmatrix} \begin{bmatrix} \tilde{p} \\ q \end{bmatrix} \quad (45)$$

The oscillating active power, $\tilde{p}$, can be obtained from the total active power using a high-pass filter. A third-order Butterworth filter with a cut-off frequency of $\omega_{ch} = 25\,\mathrm{r/s}$ is used in the tests.

On the other hand, the dc-link voltage regulation is accomplished by acting on the absorbed active power of the shunt converter. For this purpose, the dc-link voltage control loop will use an additional portion of the $i_{pq}$ current. In the following lines, the expression of the current reference, $i^{\star\mathrm{dc}}_{pq}$, is derived, which is needed to maintain the dc-link voltage in a desired value. Since the dynamics of $i_p$'s currents is faster than dc-link voltage dynamics, it can be assumed that currents are quickly stabilised. In this way, from (5) and (6), neglecting the resistive voltage drop, expressions given by (46) and (47) can be obtained.

$$\eta_{pd} v_{\mathrm{dc}} \cong L_p \omega i_{pq} + r_p(v_{fd} + v_{sd}) \quad (46)$$

$$\eta_{pq} v_{\mathrm{dc}} \cong -L_p \omega i_{pd} + r_p(v_{fq} + v_{sq}) \quad (47)$$

Then, by multiplying the dc-link voltage, $v_{\mathrm{dc}}$, with both sides of (29) and by using (46) and (47), it is possible to obtain the equation

$$i^{\star\mathrm{dc}}_{pq} \cong -\frac{C_{\mathrm{dc}} u_{\mathrm{dc}} v_{\mathrm{dc}}}{\Omega_B r_p (v_{fq} + v_{sq})} \quad (48)$$

where the series converter term has been neglected in order to avoid the filtered harmonics move from the series side to the shunt converter side. Moreover, the dc-link voltage will contain harmonics because of the UPQC smoothing action over voltages and currents. For this reason, some harmonics arise in the dc-link voltage. The auxiliary control input, $u_{\mathrm{dc}}$, is calculated from (49), with a reference value equal to the desired dc-link voltage

$$u_{\mathrm{dc}} = -K_{\mathrm{dc}}(v_{\mathrm{dc}} - v^{\star}_{\mathrm{dc}}) - \frac{K_{\mathrm{dc}}}{T_{i\mathrm{dc}}}\int (v_{\mathrm{dc}} - v^{\star}_{\mathrm{dc}})\mathrm{d}t \quad (49)$$

The $i^{\star\mathrm{dc}}_{pq}$ current should be added to the $i^{\star}_{pq}$ current, calculated in (45), to obtain the total current reference. Then, through these current references, it is possible to calculate the auxiliary control inputs $u_{pd}$ and $u_{pq}$ by following the procedure described in Subsection 4.3.

### 4.8 Non-linear transformation to obtain the IGBT gate driving signals

The original control input $\eta_p$, which represents the duty cycle of the shunt VSC, can be recovered from (27) and (28),




doi: 10.1049/iet-pel.2010.0134

resulting in

$$\eta_{pd} = \frac{1}{v_{\rm dc}}\left(R_p i_{pd} + L_p \omega i_{pq} + r_p(v_{fd} + v_{sd}) + \frac{L_p u_{pd}}{\Omega_B}\right) \quad (50)$$

$$\eta_{pq} = \frac{1}{v_{\rm dc}}\left(R_p i_{pq} - L_p \omega i_{pd} + r_p(v_{fq} + v_{sq}) + \frac{L_p u_{pq}}{\Omega_B}\right) \quad (51)$$

The amplitude and phase required for the SVM stage are calculated in an analogous way is as done in (43) and (44).

## 5 Control strategy for UPQC$_B$

### 5.1 Input transformation

As was seen in the above section with regard to the UPQC$_A$ case, here the following auxiliary control inputs are chosen in order to accomplish an exact linearisation of the UPQC$_B$ and transform the original system in a linear and decoupled system.

$$u_{sd} \triangleq \frac{\Omega_B}{L_s}\left(\frac{r_s(v_{ld} - v_{fd})}{2} - \frac{r_s(v_{lq} - v_{fq})}{2\sqrt{3}} - R_s i_{sd} - L_s \omega i_{sq} - \eta_{sd} v_{\rm dc}\right) \quad (52)$$

$$u_{sq} \triangleq \frac{\Omega_B}{L_s}\left(\frac{r_s(v_{lq} - v_{fq})}{2} + \frac{r_s(v_{ld} - v_{fd})}{2\sqrt{3}} - R_s i_{sq} + L_s \omega i_{sd} - \eta_{sq} v_{\rm dc}\right) \quad (53)$$

$$u_{pd} \triangleq \frac{\Omega_B}{L_p}\left(\frac{r_p v_{ld}}{2} - \frac{r_p v_{lq}}{2\sqrt{3}} - R_p i_{pd} - L_p \omega i_{pq} + \eta_{pd} v_{\rm dc}\right) \quad (54)$$

$$u_{pd} \triangleq \frac{\Omega_B}{L_p}\left(\frac{r_p v_{ld}}{2} + \frac{r_p v_{lq}}{2\sqrt{3}} - R_p i_{pd} + L_p \omega i_{pq} + \eta_{pd} v_{\rm dc}\right) \quad (55)$$

$$u_{vd} \triangleq \frac{\Omega_B}{3C_p}\left(-\frac{r_s i_{sd}}{2} - \frac{r_s i_{sq}}{2\sqrt{3}} - \frac{r_p i_{pd}}{2} - \frac{r_p i_{pq}}{2\sqrt{3}} - i_{ld} - 3C_p \omega v_{lq}\right) \quad (56)$$

$$u_{vq} \triangleq \frac{\Omega_B}{3C_p}\left(-\frac{r_s i_{sq}}{2} + \frac{r_s i_{sd}}{2\sqrt{3}} - \frac{r_p i_{pq}}{2} + \frac{r_p i_{pd}}{2\sqrt{3}} - i_{lq} + 3C_p \omega v_{ld}\right) \quad (57)$$

$$u_{\rm dc} \triangleq \frac{\Omega_B}{C_{\rm dc}}((\eta_{sd} i_{sd} + \eta_{sq} i_{sq}) - (\eta_{pd} i_{pd} + \eta_{pq} i_{pq})) \quad (58)$$

By replacing the auxiliary control inputs (52)–(58) in the UPQC$_B$ system, (8)–(14), the following seven first-order linear, fully actuated and decoupled systems are achieved.

$$\begin{aligned} \frac{{\rm d}i_{sd}}{{\rm d}t} &= u_{sd}, & \frac{{\rm d}i_{sq}}{{\rm d}t} &= u_{sq} \\ \frac{{\rm d}i_{pd}}{{\rm d}t} &= u_{pd}, & \frac{{\rm d}i_{pq}}{{\rm d}t} &= u_{pq} \\ \frac{{\rm d}v_{ld}}{{\rm d}t} &= u_{vd}, & \frac{{\rm d}v_{lq}}{{\rm d}t} &= u_{vq} \\ \frac{{\rm d}v_{\rm dc}}{{\rm d}t} &= u_{\rm dc} \end{aligned} \quad (59)$$

### 5.2 Load voltage control of the shunt VSC

The load voltage reference ($v_l^\star$) is designed to obtain a harmonic- and flicker-free voltage whose amplitude equals to one at the load terminal ($V_L = 1$ pu). In addition, the load terminal voltage must have the phase determined by the loss minimisation criterion from (20). Therefore

$$v_{ldq}^\star = \begin{bmatrix} v_{ld}^\star & v_{lq}^\star \end{bmatrix}^{\rm T} = \begin{bmatrix} V_L \sin\theta_L^\star & V_L \cos\theta_L^\star \end{bmatrix}^{\rm T} \quad (60)$$

Then, using these voltage references, it is possible to calculate the auxiliary control inputs, $u_{vd}$ and $u_{vq}$, in way similar to that of (35) and (36).

### 5.3 Current control of the shunt VSC

The $i_p$ current control is an inner control loop that allows for control of the $v_l$ outer voltage loop in a cascade manner. Its references are obtained from (56) and (57)

$$i_{pd}^\star = \frac{1}{2r_p}\left(-3i_{ld} + \sqrt{3}i_{lq} - 2r_s i_{sd} - 3C_p\left(\frac{3}{\Omega_B}u_{vd} - \frac{\sqrt{3}}{\Omega_B}u_{vq} + \left(\sqrt{3}v_{ld} + 3v_{lq}\right)\omega\right)\right) \quad (61)$$

$$i_{pq}^\star = \frac{-1}{2r_p}\left(3i_{lq} + \sqrt{3}i_{ld} + 2r_s i_{sq} + 3C_p\left(\frac{3}{\Omega_B}u_{vq} + \frac{\sqrt{3}}{\Omega_B}u_{vd} - (3v_{ld} - \sqrt{3}v_{lq})\omega\right)\right) \quad (62)$$

Finally from the above current references, the auxiliary control inputs $u_{pd}$ and $u_{pq}$ are calculated.

### 5.4 Non-linear transformation to obtain the IGBT gate driving signals

The original control input $\eta_p$, which represents the duty cycle of the shunt VSC, can be recovered from (54) and (55). It

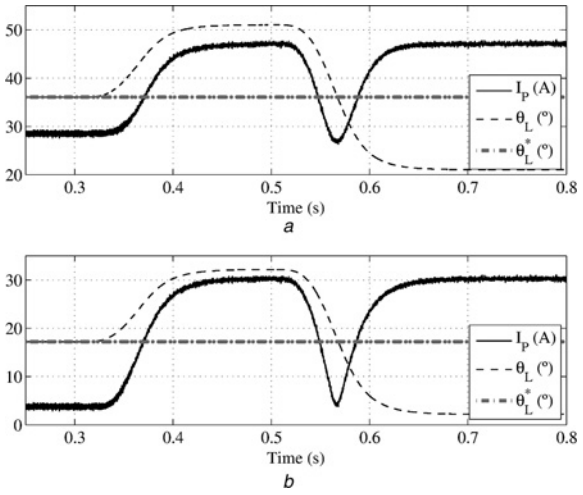


**Fig. 6** *Shunt current amplitude (solid line) and load voltage angle (dashed line) for the optimal operation test*

*a* UPQC$_A$ case
*b* UPQC$_B$ case

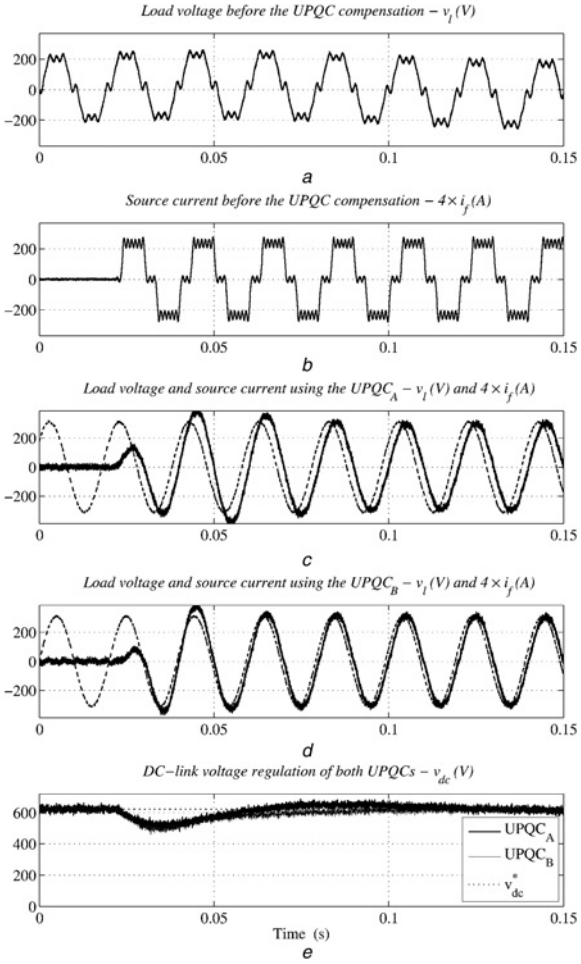


**Fig. 7** *UPQC filter task*

*a* and *b* Load voltage and source current before the UPQC compensation
*c* and *d* Load voltage and source current using the UPQC$_A$ and UPQC$_B$, respectively
*e* dc-link voltage regulation

becomes

$$\eta_{pd} = \frac{1}{v_{\mathrm{dc}}}\left(-\frac{r_p}{2}v_{ld} + \frac{r_p}{2\sqrt{3}}v_{lq} + R_p i_{pd} + L_p \omega i_{pq} + \frac{L_p}{\Omega_B}u_{pd}\right) \quad (63)$$

$$\eta_{pq} = \frac{1}{v_{\mathrm{dc}}}\left(-\frac{r_p}{2}v_{lq} - \frac{r_p}{2\sqrt{3}}v_{ld} + R_p i_{pq} - L_p \omega i_{pd} + \frac{L_p}{\Omega_B}u_{pq}\right) \quad (64)$$

### 5.5 Control current of the series VSC

A PI control is implemented to calculate the current reference, $i^\star_{fq}$. By means of this control, the dc-link voltage regulation is also attained

$$i^\star_{fq} = -K_B(v_{\mathrm{dc}} - v^\star_{\mathrm{dc}}) - \frac{K_B}{T_{iB}}\int (v_{\mathrm{dc}} - v^\star_{\mathrm{dc}})\mathrm{d}t \quad (65)$$

The bandwidth of this control loop should be designed such that the current flowing through the series converter does not present undesired high-order harmonics. Consequently the $i_f$ current at the network input terminal shall have a low total harmonic distortion index. On the other hand, in order to achieve a unity power factor at the UPQC input, the reactive current component should be nullified, hence

$$i^\star_{fd} = 0 \quad (66)$$

By applying the first Kirchhoff law in the transformer triangle of the series converter, it can be shown that the $i^\star_s$ current reference, in terms of the previously calculated $i^\star_f$ current, will be

$$i^\star_{sdq} = \begin{bmatrix} i^\star_{sd} & i^\star_{sq} \end{bmatrix}^{\mathrm{T}} = \begin{bmatrix} \dfrac{\sqrt{3}i^\star_{fq}}{2r_s} & \dfrac{-3i^\star_{fq}}{2r_s} \end{bmatrix}^{\mathrm{T}} \quad (67)$$

Finally the auxiliary control inputs $u_{sd}$ and $u_{sq}$ are calculated from the $i^\star_{sdq}$ current references.

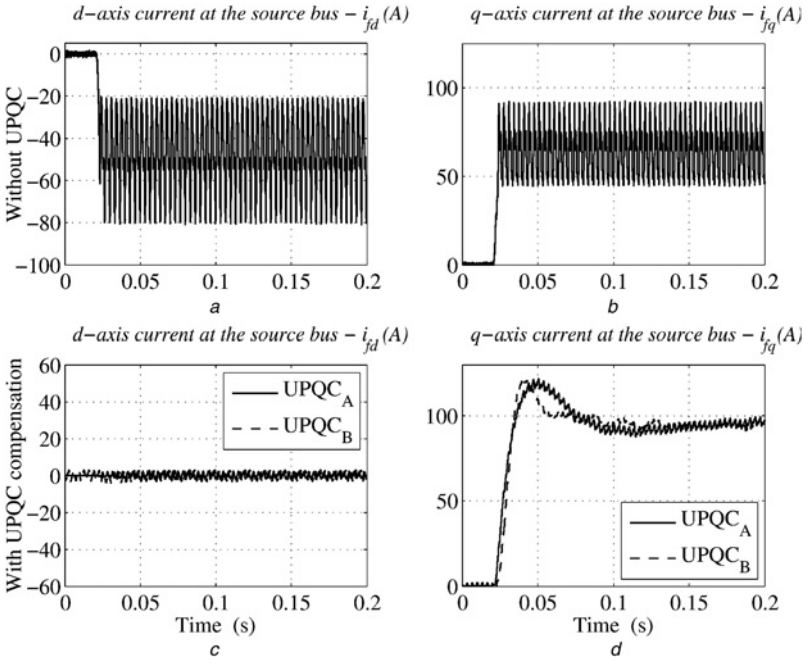


**Fig. 8** *Transient response against a load step*

*a* and *b* *d*- and *q*-axis current at the source bus without UPQC compensation
*c* and *d* *d*- and *q*-axis current at the source bus with UPQC compensation




doi: 10.1049/iet-pel.2010.0134

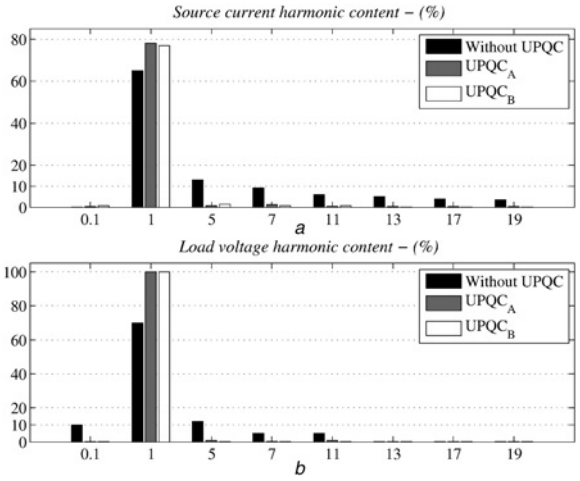


**Fig. 9** *Harmonic content with and without UPQC compensation*

*a* Source current harmonic content
*b* Load voltage harmonic content

### 5.6 Non-linear transformation to obtain the IGBT gate driving signals

Duty cycles of the series VSC can be recovered from (52) and (53), yielding

$$\eta_{sd} = \frac{1}{v_{\mathrm{dc}}}\left(\frac{1}{2}r_s(v_{ld} - v_{fd}) - \frac{1}{2\sqrt{3}}r_s(v_{lq} - v_{fq}) - R_s i_{sd} - L_s\omega i_{sq} - \frac{L_s}{\Omega_B}u_{sd}\right) \tag{68}$$

$$\eta_{sq} = \frac{1}{v_{\mathrm{dc}}}\left(\frac{1}{2}r_s(v_{lq} - v_{fq}) + \frac{1}{2\sqrt{3}}r_s(v_{ld} - v_{fd}) - R_s i_{sq} + L_s\omega i_{sd} - \frac{L_s}{\Omega_B}u_{sq}\right) \tag{69}$$

Finally the amplitude and phase required for the SVM stage are calculated in way similar to that in (43) and (44).

## 6 UPQC comparison

This section summarises main differences of both UPQC topologies.

- UPQC$_A$ uses the series converter as a non-sinusoidal voltage source and the shunt converter as a non-sinusoidal current source. On the other hand, UPQC$_B$ uses the shunt converter as a sinusoidal voltage source and the series converter as a sinusoidal current source.
- UPQC$_B$ control strategy has a simpler control implementation, from the reference calculation point of view, because filters are not necessary for harmonic extraction.
- In UPQC$_B$ topology, when $C_p$ capacitors are negligible, $I_R \cong 0$ is verified and consequently $\theta_L^{\star} \cong \phi$. From this point of view, (16) is a particular case of (20).
- Different to UPQC$_A$ philosophy, where dc-link voltage is regulated by the shunt VSC, in UPQC$_B$ philosophy the series VSC is used to maintain the dc-link voltage in a desired value.
- It is worth noting that the optimal angle in the case of both strategies (see (16) and (20) and Fig. 6) is not the same, even under equal load and network voltage conditions. This is because of the different connections, which in the load bus for each UPQC, produce a different filter topology.

## 7 Performance assessment

The most relevant results demonstrating the performance of the proposed optimal strategy and a comparison of UPQC$_A$'s and UPQC$_B$'s philosophies are presented in this

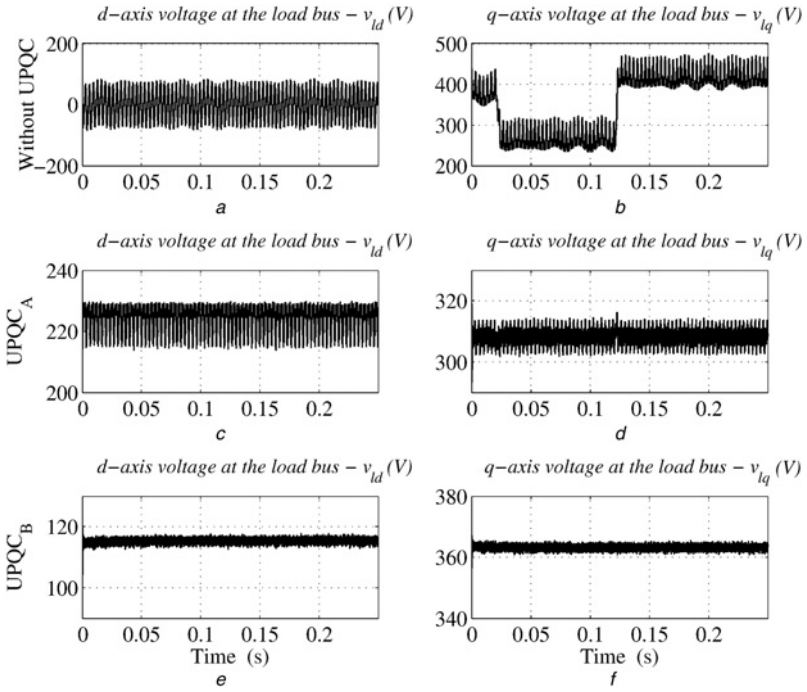


**Fig. 10** *Input-voltage variation test*

*a* and *b* *d*- and *q*-axis voltage at the load bus without UPQC compensation
*c* and *d* *d*- and *q*-axis voltage at the load bus using the UPQC$_A$
*e* and *f* *d*- and *q*-axis voltage at the load bus using the UPQC$_B$

section. The UPQC, VSCs and control strategy are implemented using the SimPowerSystems blockset of MATLAB®. The power system configuration and parameters used in the tests are displayed in Fig. 1 and Table 1.

### 7.1 UPQC optimal operation

The following test has been carried out to show how, by minimising the shunt converter current, the UPQC works at the optimal operation point. For the sake of simplicity, harmonics are not considered in this test. Both UPQCs work at nominal load, with a network voltage reduced to 70% of the nominal value. Fig. 6 shows how, at the beginning, both controllers are placed with the load voltage angle equal to the optimal value. Then, the $\theta_L$ angle is swept in $\pm 15^{\circ}$ around the operation point; it can be seen that when the $\theta_L$ angle moves away from the optimal point, the shunt VSC current grows in both directions. Moreover, at 0.58 s, when the load voltage angle crosses over the optimal value, the minimal $I_P$ current is consumed. This shows that any other value chosen in case of $\theta_L$ makes the $I_P$ current higher and, consequently, the converter losses are higher as well.

### 7.2 Dynamic response against sudden load changes

A highly distorted input voltage has been considered in this test, with a 30% nominal value decrease and flicker of 6 Hz with 10% of the fundamental amplitude (see Fig. 7*a*). A six-pulse thyristor rectifier is used as the load. At 0.02 s, the UPQC is suddenly loaded to the nominal value (see Fig. 7*b*). The UPQC filter task is shown in Figs. 7*b* and *c*. There, it can be seen that both the load voltage and source current, are properly compensated for. Fig. 7*d* shows the dc-link regulation. In Fig. 8 the transient response against a step change in the load power, with and without UPQC compensations, is depicted.

The source current and the load voltage harmonic content are presented in Fig. 9. It can be seen that the flicker and harmonics are substantially reduced, whereas the fundamental load voltage is restored to its nominal value, in both $\text{UPQC}_A$ and $\text{UPQC}_B$ cases.

### 7.3 Compensation of input-voltage variations

In this test the same distorted nominal load, harmonics, and input-voltage flicker, as seen in previous tests, were

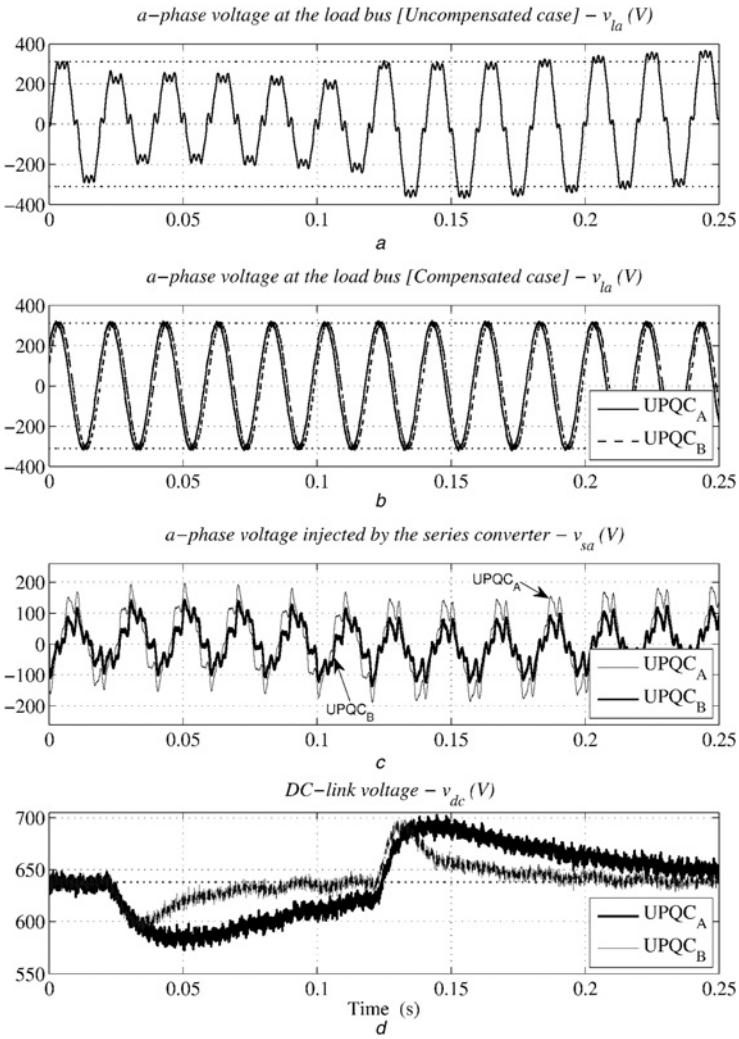


**Fig. 11** *Load terminal voltage wave form before and after the compensation*

*a* Load voltage without compensation
*b* Load voltage with both proposed UPQCs compensations
*c* Series voltage injected by each UPQC topology
*d* dc-link voltage regulation




doi: 10.1049/iet-pel.2010.0134

considered. However, in this case, a 30% reduction in the input-voltage at 0.02 s and a 10% elevation over the nominal value at 0.12 s are introduced. Fig. 10 shows the performance of both strategies, where the load terminal voltage in the $d-q$ reference frame, before and after the compensation, can be seen. Both controllers compensate for the input-voltage variations properly; nevertheless, the UPQC$_A$ is not capable of eliminating completely the ripple in the load voltage, whereas the UPQC$_B$ is more effective in maintaining an almost constant load voltage.

The flicker level, harmonics and amplitude variations in a phase input-voltage of the non-compensated case are shown in Fig. 11*a*. In Fig. 11*b*, it can be seen that all these disturbances are mitigated when the UPQC compensation is used. A phase shift is also noted, depending on which optimal control philosophy is applied.

In Fig. 11*c* it can be seen that the UPQC$_B$ needs a lower injected voltage to restore the load voltage at the nominal value. When the optimal angle calculated in the case of each topology is observed (see Fig. 6), it can be seen that a lower voltage phase shift is required in the UPQC$_B$'s case. The UPQC$_A$ optimal angle is the load power factor angle ($36^\circ$ in this test); whereas in the UPQC$_B$, from (20), the optimal angle is $19^\circ$. This indicates that lesser effort is needed by the UPQC$_B$ in order to work at the optimal point. For this reason, the UPQC$_B$ allows for the compensation of larger range of sags than does the UPQC$_A$, when the same nominal voltage of the series converter is considered.

In Fig. 11*d* a value of dc-voltage setting time for UPQC$_A$ case is observed. This is higher than UPQC$_B$. The UPQC$_A$ setting time can be reduced, making the dc-voltage control loop faster. However this diminishes the harmonic elimination capacity of the shunt converter. This is because of the trade-off between current harmonic filtering and dc-voltage regulation in both, *A* and *B*, philosophies. Finally both non-linear controllers are able to regulate the dc-link voltage. Although dc-voltage variations occur transiently, they can continue their power quality-improving tasks in a suitable way.

## 8 Conclusions

In this paper a new optimal strategy with regard to UPQCs is proposed. The optimal strategy was chosen to minimise the loss power consumption. A comparison of two UPQC control philosophies is also presented. With regard to current and voltage harmonic compensation, unity power factor condition and dc-voltage regulation, both control philosophies present a good performance. Therefore the non-linear control for UPQC could have a very important role in the electric network power quality. However, there are remarkable differences between both UPQC control strategies presented in this work. Firstly the optimal strategy proposed in the case of the UPQC$_B$ has a simpler control implementation, from the reference calculation point of view, as filters are not necessary for harmonic extraction. This allows for a fast dynamic response against sudden load changes and input voltage variations. In order to obtain the same dynamic response with the UPQC$_A$, filters and in reference calculation must be faster but, as a consequence, this lead to its harmonic elimination characteristic being deteriorated. Thus, it can be concluded that the UPQC tuning is a trade-off between transient response and harmonic elimination, where UPQC$_B$, in case of the same transient response speed against load steps, presents less harmonic content. Additionally the relation 'dc-voltage regulation performance' against 'current harmonic elimination' is more efficient when UPQC$_B$ is used, at least in terms of the application analysed here. Finally the UPQC$_B$'s philosophy with the optimal non-linear control proposed in this work, leads to a better performance than the other UPQC option generally found in literature.

## 9 References


1 Bollen, M.H.: 'Understanding power quality problems: voltage sags and interruptions' (Wiley-IEEE Press, 1999)
2 Luo, A., Shuai, Z., Zhu, W., Shen, Z.J., Tu, C.: 'Design and application of a hybrid active power filter with injection circuit', *IET Power Electron.*, 2010, **3**, (1), pp. 54–64
3 Garg, V., Singh, B., Bhuvaneswari, G.: '24-pulse ac–dc converter for harmonic mitigation', *IET Power Electron.*, 2009, **2**, (4), pp. 364–374
4 Mendalek, N., Al-Haddad, K., Fnaiech, F., Dessaint, L.A.: 'Nonlinear control technique to enhance dynamic performance of a shunt active power filter', *IEE Proc Electr. Power Appl.*, 2003, **150**, (4), pp. 373–379
5 Hua, C.-C., Li, C.-H., Lee, C.-S.: 'Control analysis of an active power filter using lyapunov candidate', *IET Power Electron.*, 2009, **2**, (4), pp. 325–334
6 Sawant, R.R., Chandorkar, M.C.: 'Methods for multi-functional converter control in three-phase four-wire systems', *IET Power Electron.*, 2009, **2**, (1), pp. 52–66
7 Peterson, M., Singh, B.N.: 'Multipulse controlled ac/dc converters for harmonic mitigation and reactive power management', *IET Power Electron.*, 2009, **2**, (4), pp. 443–455
8 Leon, A.E., Mauricio, J.M., Solsona, J.A., Gomez-Exposito, A.: 'Software sensor-based STATCOM control under unbalanced conditions', *IEEE Trans. Power Deliv.*, 2009, **24**, (3), pp. 1623–1632
9 Vodyakho, O., Kim, T.: 'Shunt active filter based on three-level inverter for three-phase four-wire systems', *IET Power Electron.*, 2009, **2**, (3), pp. 216–226
10 Fujita, H., Akagi, H.: 'The unified power quality conditioner: the integration of series and shunt-active filters', *IEEE Trans. Power Electr.*, 1998, **13**, (2), pp. 315–322
11 Ghosh, A., Ledwich, G.: 'A unified power quality conditioner (UPQC) for simultaneous voltage and current compensation', *Electr. Power Syst. Res.*, 2001, **59**, (1), pp. 55–63
12 Khoor, M.S., Machmoum, M., Abdelli, Y.: 'Using a simple analogical identification method and PID controllers for unified power quality conditioning'. European Conf. on Power Electronics and Application, September 2005, pp. 1–10
13 Sepulveda, C.A., Espinoza, J.R., Moran, L.A., Ortega, R.: 'Analysis and design of a linear control strategy for three-phase UPQCs'. 30th Annual Conf. on IEEE Industrial Electronics Society, IECON'04, November 2004, vol. 3, pp. 3060–3065
14 Li, P., Bai, Q., Li, G.: 'Coordinated control strategy for UPQC and its verification'. IEEE Power Engineering Society General Meeting, June 2006, pp. 1–8
15 Elmitwally, A., Abdelkader, S., Elkateb, M.: 'Universal power quality manager with a new control scheme', *IEE Proc. Gener. Transm. Distrib.*, 2000, **147**, (3), pp. 183–189
16 Ming, Z., Jian-Ru, W., Zhi-Qiang, W., Jian, C.: 'Control method for power quality compensation based on levenberg-marquardt optimized BP neural networks'. CES/IEEE Fifth Int. Power Electronics and Motion Control Conf., IPEMC'06, August 2006, vol. 3, pp. 1–4
17 Ramirez, S., Visairo, N., Oliver, M., Nunez, C., Cardenas, V., Sira-Ramirez, H.: 'Harmonic compensation in the AC mains by the use of current and voltage active filters controlled by a passivity-based law'. Seventh IEEE Int. Power Electronics Congress, CIEP'00, October 2000, pp. 87–92
18 Kolhatkar, Y.Y., Errabelli, R.R., Das, S.P.: 'A sliding mode controller-based optimum UPQC with minimum VA loading'. IEEE Power Engineering Society General Meeting, June 2005, vol. 1, pp. 871–875
19 Hongchun, S., Zuquan, L., Jilai, Y., Liang, X.: 'A novel control strategy for UPQC'. IEEE/PES Transmission and Distribution Conf. and Exhibition: Asia and Pacific, 2005, pp. 1–4
20 Basu, M., Farrell, M., Conlon, M.F., Gaughan, K., Coyle, E.: 'Optimal control strategy of UPQC for minimum operational losses'. 39th Int. Universities Power Engineering Conf., UPEC'04, September 2004, vol. 1, pp. 246–250
21 Faranda, R., Valade, I.: 'UPQC compensation strategy and design aimed at reducing losses'. IEEE Int. Symp. Industrial Electronics, ISIE'02, July 2002, vol. 4, pp. 1264–1270

22 Kolhatkar, Y.Y., Das, S.P.: 'Experimental investigation of a single-phase UPQC with minimum VA loading', *IEEE Trans. Power Deliv.*, 2007, **22**, (1), pp. 373–380

23 Kolhatkar, Y.Y., Das, S.P.: 'Simulation and experimental investigation of an optimum UPQC with minimum VA loading'. Int. Conf. on Power Electronics and Drives Systems, PEDS'05, 2005, vol. 1, pp. 526–531

24 Yun, M.-S., Lee, W.-C., Suh, I., Hyun, D.-S.: 'A new control scheme of unified power quality compensator-Q with minimum power injection'. 30th Annual Conf. on IEEE Industrial Electronics Society, IECON'04, 2004, vol. 1, pp. 51–56

25 Esfandiari, A., Parniani, M., Mokhtari, H.: 'Mitigation of electric arc furnace disturbances using the unified power quality conditioner'. 30th Annual Conf. on IEEE Industrial Electronics Society, IECON'04, November 2004, vol. 2, pp. 1469–1474

26 Ryoo, H.-J., Rim, G.-H., Kim, T.-J., Kisck, D.O.: 'Digital-controlled single-phase unified power quality conditioner nonlinear and voltage sensitive load'. 30th Annual Conf. on IEEE Industrial Electronics Society, IECON'04, November 2004, vol. 1, pp. 24–29

27 Khadkikar, V., Agarwal, P., Chandra, A., Barry, A.O., Nguyen, T.D.: 'A simple new control technique for unified power quality conditioner (UPQC)'. 11th Int. Conf. on Harmonics and Quality of Power, September 2004, pp. 289–293

28 Khadkikar, V., Chandra, A., Barry, A.O., Nguyen, T.D.: 'Application of UPQC to protect a sensitive load on a polluted distribution network'. IEEE Power Engineering Society General Meeting, June 2006, pp. 1–6

29 Ng, F., Wong, M.-C., Han, Y.-D.: 'Analysis and control of UPQC and its DC-link power by use of p-q-r instantaneous power theory'. First Int. Conf. on Power Electronics Systems and Applications, November 2004, pp. 43–53

30 Graovac, D., Katic, V., Rufer, A.: 'Power quality problems compensation with universal power quality conditioning system', *IEEE Trans. Power Deliv.*, 2007, **22**, (2), pp. 968–976

31 Han, B., Bae, B., Kim, H., Baek, S.: 'Combined operation of unified power-quality conditioner with distributed generation', *IEEE Trans. Power Deliv.*, 2006, **21**, (1), pp. 330–338

32 Chen, G., Chen, Y., Sanchez, L.F., Smedley, K.M.: 'Unified power quality conditioner for distribution system without reference calculations'. Fourth Int. Power Electronics and Motion Control Conf., IPEMC'04, 2004, vol. 3, pp. 1201–1206

33 Tey, L.H., So, P.L., Chu, Y.C.: 'Unified power quality conditioner for improving power quality using ANN with hysteresis control'. Int. Conf. on Power System Technology, PowerCon'04, 2004, vol. 2, pp. 1441–1446

34 Zhu, P., Li, X., Kang, Y., Chen, J.: 'Control scheme for a universal power quality manager in a two-phase synchronous rotating frame', *IEE Proc. Gener. Transm. Distrib.*, 2004, **151**, (5), pp. 590–596

35 Dai, K., Liu, P., Wang, G., Duan, S., Chen, J.: 'Practical approaches and novel control schemes for a three-phase three-wire series-parallel compensated universal power quality conditioner'. Applied Power Electron. Conf. Expos., APEC'04, 2004, vol. 1, pp. 601–606

36 Oliveira da Silva, S.A., Donoso-Garcia, P., Cortizo, P.C., Seixas, P.F.: 'A line-interactive UPS system implementation with series-parallel active power-line conditioning for three-phase, four-wire systems', *Int. J. Electr. Power Energy Syst.*, 2004, **26**, (6), pp. 399–411

37 Oliveira da Silva, S.A., Donoso-Garcia, P., Cortizo, P.C., Seixas, P.F.: 'A three-phase line-interactive UPS system implementation with series-parallel active power-line conditioning capabilities', *IEEE Trans. Ind. Appl.*, 2002, **38**, (6), pp. 1581–1590

38 Dixon, J.W., Venegas, G., Moran, L.A.: 'A series active power filter based on a sinusoidal current-controlled voltage-source inverter', *IEEE Trans. Ind. Electr.*, 1997, **44**, (5), pp. 612–620

39 Akagi, H., Kanazawa, Y., Nabae, A.: 'Instantaneous reactive power compensators comprising switching devices without energy storage components', *IEEE Trans. Ind. Appl.*, 1984, **20**, (3), pp. 625–630

40 Herrera, R.S., Salmeron, P.: 'Present point of view about the instantaneous reactive power theory', *IET Power Electron.*, 2009, **2**, (5), pp. 484–495

41 Afonso, J., Couto, C., Martinsi, J.: 'Active filters with control based on the p-q theory', *IEEE Ind. Electron. Soc. Newsl.*, 2000, **47**, (3), pp. 5–10

42 Khadkikar, V., Chandra, A.: 'A new control philosophy for a unified power quality conditioner (UPQC) to coordinate load-reactive power demand between shunt and series inverters', *IEEE Trans. Power Deliv.*, 2008, **23**, (4), pp. 2522–2534

43 Khadkikar, V., Chandra, A., Singh, B.N.: 'Generalised single-phase p-q theory for active power filtering: simulation and DSP-based experimental investigation', *IET Power Electron.*, 2009, **2**, (1), pp. 67–78

44 Czarnecki, L.S.: 'Effect of supply voltage asymmetry on IRP p-q-based switching compensator control', *IET Power Electron.*, 2010, **3**, (1), pp. 11–17

45 Isidori, A.: 'Nonlinear control systems' (Springer-Verlag, London, Great Britain, 1995, 3rd edn.)

46 Leon, A.E., Solsona, J.A., Busada, C., Chiacchiarini, H., Valla, M.I.: 'High-performance control of a three-phase voltage-source converter including feedforward compensation of the estimated load current', *Energy Convers. Manage.*, 2009, **50**, (8), pp. 2000–2008

47 Lee, K., Jahns, T.M., Lipo, T.A., Blasko, V., Lorenz, R.D.: 'Observer-based control methods for combined source-voltage harmonics and unbalance disturbances in PWM voltage-source converters', *IEEE Trans. Ind. Appl.*, 2009, **45**, (6), pp. 2010–2021

48 Åström, K.J., Wittenmark, B.: 'Computer-controlled systems: theory and design' (Prentice-Hall, 1996, 3rd edn.)

49 Saeedifard, M., Nikkhajoei, H., Iravani, R.: 'A space vector modulated STATCOM based on a three-level neutral point clamped converter', *IEEE Trans. Power Deliv.*, 2007, **22**, (2), pp. 1029–1039





doi: 10.1049/iet-pel.2010.0134